Photo-Reflectance Characterization of Nanometer Scale Active Layers in Si

Will Chism[1], Daniel Pham[2], and John Allgair[2]

[1]*Xitronix Corporation, 3925 W. Braker Lane, Ste. 3.8041, Austin, TX 78759*
[2]*Freescale assignee to SEMATECH, 2706 Montopolis Drive, Austin, TX 78741*

Abstract. This paper describes the use of a new photo-reflectance metrology technique to characterize active dopant concentration and strain in silicon nanofilmstructures. This new photo-reflectance (PR) technique is highly sensitive to Si nanofilm properties such as active dopant concentration and strain through the effect of nanometer scale space charge fields induced near the semiconductor surface. Use of the technique for precision measurement of active dopant concentration in Si ultra-shallow junctions is reported. Additionally, use of this photo-reflectance technique to characterize strain in ultra-thin strained Si layers of thickness ≤ 6 nm is reported.

Keywords: Photo-Reflectance, Dopant Concentrations, Ultra-Shallow Junctions, Strain.
PACS: 71.20.–b, 78.20.–e, 78.40.–q, 78.66.–w, 78.67.–n, 81.05.–t

INTRODUCTION

Process control capability for electrically active nanostructures is an emerging high priority need in IC manufacturing. For example, the rapid and non-destructive characterization of strain in nanoscale silicon-on-insulator (SOI) layers is required by IC manufacturers introducing strained SOI at the 45 nm process node. Additionally, precision measurement of strain and active dopant is required by manufacturers introducing B doped SiGe nanostructures for PMOS transistors. The improved transistor performance driving the introduction of strain is also expected to motivate introduction of "alternate channel" materials such as Ge and GaAs. Naturally, the most attractive techniques for process control of electrically active nanostructures will be directly sensitive to *electronic* properties. However, the metrology techniques which have received the most attention from industry, such as Raman spectroscopy and XRD, do not provide this capability. Fortunately, a non-destructive photo-reflectance (PR) technique can be used to rapidly characterize active electronic properties of nanostructures. In particular, this paper describes the application of a new PR metrology technique to characterize active dopant concentration in ultra-shallow junctions and strain in ultra-thin strained Si layers. This new PR technique provides a breakthrough process control capability essential to the volume manufacture of nanoelectronics.

PRINCIPLES OF PHOTO-REFLECTANCE MEASUREMENT

Modern photo-reflectance techniques are routinely used to measure differential changes in reflectivity smaller than one part in 10^6. Accordingly, they are an ideal candidate for applications requiring measurement of small optical signals related to electronic transitions in semiconductor nanostructures. In photo-reflectance, a pump laser beam is used to periodically modulate the carrier density in a semiconductor sample, and hence modulate one or more physical quantities, such as internal electric fields, interband transition energies, and/or temperature, thereby inducing a periodic variation in the reflectivity of the sample, which is then recorded by use of a coincident probe light beam. Generally, the photo-reflectance signal may be written:

$$\Delta R/R = \alpha\Delta\varepsilon_1 + \beta\Delta\varepsilon_2, \qquad (1)$$

where $\Delta R/R$ is the normalized change in reflectivity, $\alpha \equiv \partial(\ln R)/\partial\varepsilon_1$ and $\beta \equiv \partial(\ln R)/\partial\varepsilon_2$ are the "Seraphin coefficients" which contain filmstack information, and $\Delta\varepsilon_1$ and $\Delta\varepsilon_2$ are the pump induced changes in the real and imaginary parts of the dielectric function, respectively [1, 2]. Effective application of PR to process control in semiconductor nano-manufacturing then depends on i) the ability of the pump to induce changes in the dielectric function of the nanostructures of interest, and related to the electrical performance of

the nanostructures, ii) the sensitivity of the probe to said changes, and iii) the practical realization of process control criteria such as high measurement speed, repeatability, spot size, etc.

In order to appreciate these constraints, it is instructive to consider an industry accepted process control application of PR. Historically, implant monitoring in Si IC manufacturing has been accomplished with a PR technique using a 488 nm wavelength laser pump beam in conjunction with a 633 nm laser probe. A pump laser beam of several milliwatts is focused to a micron spot on a silicon wafer, producing an induced charge density on the order $10^{18}/cm^3$ [3]. The presence of carriers modifies the silicon dielectric function through the addition of a Drude plasma term and through a small temperature rise. At the 633 nm probe wavelength, only changes in the real part of the Si dielectric function are significant. The PR signal is then just $\Delta R/R \cong \alpha\Delta\varepsilon_1$. The implant layer can be modeled with an effective medium approximation consisting of amorphous silicon (damage) and crystalline silicon. To calculate α, we may first derive an analytical expression for R in terms of the indices of refraction of the damage layer and substrate, and the thickness of the damage layer. This may also be done numerically, and for any angle of incidence or polarization condition. Then R may be numerically differentiated with respect to the real part of the dielectric function, and α constructed. Generally, the Seraphin coefficients will oscillate with a period of $4\pi nd/\lambda$, where n is the index of refraction on the damage layer, d is the thickness of the damage layer, and λ is the probe beam wavelength. The periods of these cosine-like curves have been fit in attempts to extract junction depth [4, 5]. Fig. 1 shows the dependence of the Seraphin coefficient α on the damage layer depth and damage fraction, for the 633 nm probe wavelength. The top, middle, and bottom curves correspond to 10%, 30%, and 50% amorphization of the implanted layer, respectively. The Seraphin coefficient is $\alpha \approx 4\times10^{-2}$, while the change in the dielectric function due to the Drude carrier plasma is $\Delta\varepsilon_1 \approx -3\times10^{-3}$, producing a plasma contribution to the PR signal of $\Delta R/R \cong -1\times10^{-4}$. As it turns out, the thermal term is of opposite sign and nearly cancels the plasma contribution, resulting in observed signals on the order 1×10^{-5} or less [3]. Despite the low signal levels, this historical implementation of PR has provided effective process control in implant process control applications in IC manufacturing for over two decades. However, due to the 633nm wavelength being far from any significant optical features in silicon, the probe has no sensitivity to internal electric fields and/or interband transition energies. As shown below, this prevents the technology from being able to distinguish between active and inactive dopant, and also precludes any sensitivity to strain.

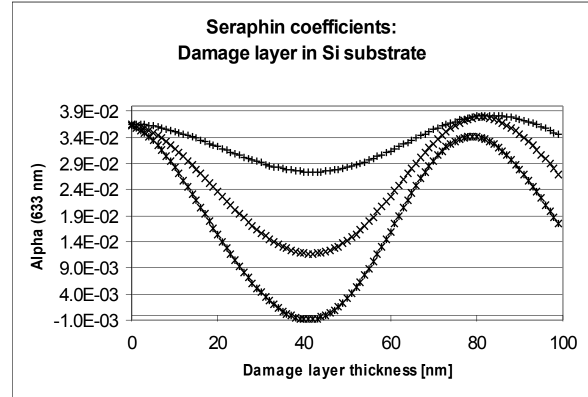

FIGURE 1. Calculated Seraphin coefficient $\alpha=\partial(\ln R)/\partial\varepsilon_1$, at λ = 633 nm, of a thin implant damage layer in a silicon substrate, as a function of implant dose and depth.

In contrast with this historical application of PR to implant monitoring, the PR metrology technique discussed herein attains sensitivity to the active electronic properties of Si nanostructures by using a probe wavelength near the "E_1" interband transition in Si, which occurs at a wavelength of approximately 375 nm. In the vicinity of such a transition, the induced changes in the dielectric function $\Delta\varepsilon_1$ and $\Delta\varepsilon_2$ may be written as the product of the free carrier energy and a third derivative of the semiconductor dielectric function: $\Delta\varepsilon_i = \partial^3(\omega\varepsilon_i)/\partial\omega^3 \times U_F$, where U_F is the free carrier energy and ω is the photon frequency [6]. Thus, one motivation for choosing the wavelength of the probe beam at 375 nm for Si lies in the sharp derivative form for $\Delta\varepsilon_1$ and $\Delta\varepsilon_2$. The total PR signal then becomes:

$$\Delta R/R = \mathrm{Re}[(\alpha - i\beta)\times\partial^3(\omega\varepsilon)/\partial\omega^3)]\times U_F. \quad (2)$$

The third derivative functional form is large only nearby strong optical absorptions in the semiconductor band structure, and thus may isolate these features with great precision. This is what allows the PR technique to precisely measure strain in nanoscale strained silicon layers, for example, since the Si E_1 transition energy undergoes a known shift under strain. Nearby to these strong optical absorptions, the amplitude of the PR response also has excellent sensitivity to electric fields in activated silicon transistor channel regions: note the free carrier energy is given by the expression $U_F = e^2h^2F^2/24m\omega^2$, where e is the electronic charge, h is Plank's constant, F is the space charge field, and m is the effective mass [6]. This free carrier energy is also proportional to the induced carrier density, which may be seen from the

Poisson relation: $N_e = \varepsilon_o F^2/2eV$, where N_e is the carrier density, V is the built-in surface voltage and ε_o is the permittivity of the material [2, 6]. FIG. 2 shows the calculated PR signal near the Si E_1 interband transition energy for a pump induced space charge field of F = 430kV/cm, which roughly corresponds to a carrier density of $N_e \approx 10^{18}/cm^3$. As seen in FIG. 2, in the wavelength range of 360-380 nm, the amplitude of this signal becomes two orders of magnitude larger than the PR signals achieved in implant monitoring systems (for the same pump conditions). Moreover, by reason of the fact that the PR signal is highly sensitive to the near surface crystallinity, it may be used to precisely measure activated dopant in Si transistor channels.

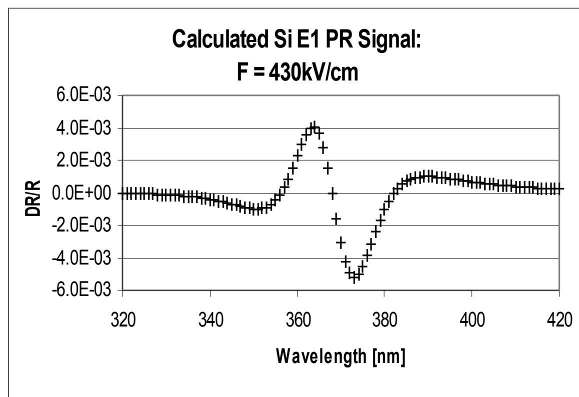

FIGURE 2. Calculated PR signal near the Si E_1 interband transition energy, for a pump induced space charge field of 430kV/cm.

CHARACTERIZATION OF ACTIVE DOPANT IN ULTRA-SHALLOW JUNCTIONS

In order to evaluate the sensitivity of PR technique to doping levels in ultra-shallow junctions, the International SEMATECH Manufacturing Initiative generated a set of arsenic implanted silicon wafers with varying implant dose and implant energies. The process matrix used 24 wafers, with dose and depth targeted to approximate implant specifications at the 65 to 45 nm nodes. The implant ion energies were varied to provide four implant depths of approximately 10, 20, 30, and 40 nm. Each of the DoE target depths further comprised three dose splits producing nominal doping densities of approximately 10^{18}, 10^{19}, and 10^{20} atoms/cm^3. Finally, an anneal split was performed comprising an anneal of 5 seconds at 1000°C. This anneal was intended to result in complete activation irrespective of dose and density conditions. No attempt to minimize dopant diffusion was made.

At the 375 nm probe wavelength changes in both the real and imaginary part of the Si dielectric function are significant. FIG. 3 shows the dependence of the Seraphin coefficient β on the damage layer depth and damage fraction, for the 375 nm probe wavelength. The top (+), middle (×), and bottom curves correspond to 10%, 30%, and 50% amorphization, respectively. The shorter period of oscillation of the Seraphin coefficients at 375 nm, as compared to the 633 nm wavelength of FIG. 1, demonstrates this wavelength will exhibit improved sensitivity to smaller junction depths. Additionally, the dampening of the cosine-like curves due to absorption at 375 nm indicates this wavelength is sensitive only to the first ~80 nm from the silicon surface, at most.

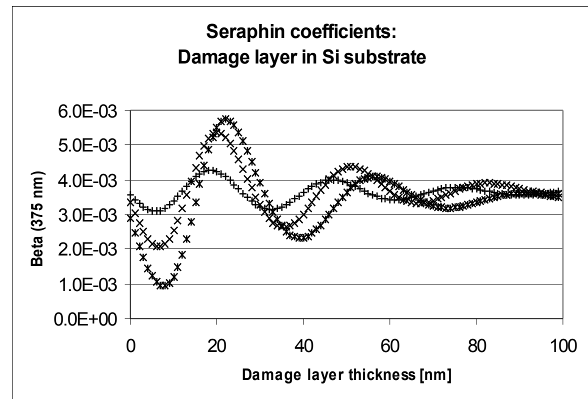

FIGURE 3. Calculated Seraphin coefficient $\beta = \partial(\ln R)/\partial\varepsilon_2$, at λ = 375nm, of a thin implant damage layer in a silicon substrate, as a function of implant dose and depth.

The prototype PR system was configured with pump and probe wavelengths of 844 nm and 374 nm, respectively. The pump intensity of approximately 15 mW was amplitude modulated with a 2 MHz square wave. The pump and probe were co-focused to a 6.5 micron spot on the surface of each wafer. The reflected probe light was passed through a color filter to eliminate the pump light, and projected onto a photodiode where its intensity was recorded using phase locked detection. The measurement itself takes approximately one second. For the pump wavelength and focusing conditions, the carrier density generated is at least two orders of magnitude smaller than used in commercial implant monitoring systems, or $N_e \leq 10^{16}/cm^3$. However, the greatly enhanced sensitivity of the 375 nm probe counteracts the reduced pump intensity, resulting in signal levels commensurate with levels in existing production systems.

Fig. 4 shows the modulus of the experimental PR signal for the annealed samples, as a function of junction depth. For each junction depth, the modulus of the PR signal $|\Delta R/R|$ rises approximately one order of magnitude for a two decade change in dose. This demonstrates excellent sensitivity to active dopant concentration for the ultra-shallow junction depths expected at the 45 nm node. It may also be seen that

the data is highly reproducible. In fact, measurement precision has been established at ~5×10^{-7} for the prototype system. It is also seen each of the three "rows" in Fig. 4 exhibit a sinusoidal variation with junction depth—this is just the expected filmstack dependence (contained in the Seraphin coefficients).

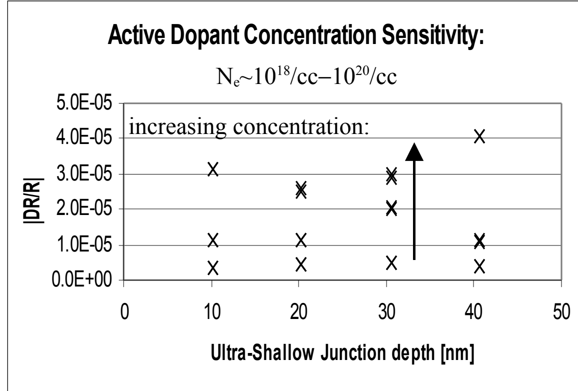

FIGURE 4. Modulus of the experimental PR signal at λ = 374 nm obtained from nanometer scale active layers in Si, as a function of ultra-shallow junction depth.

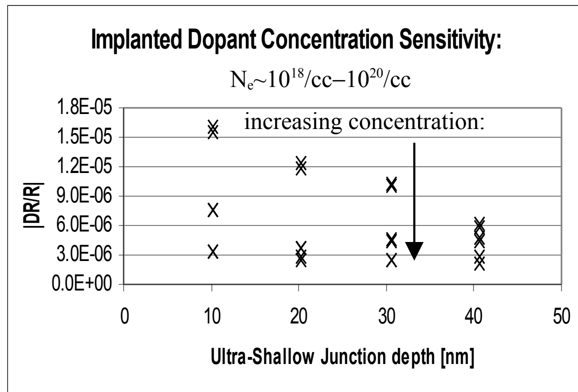

FIGURE 5. Modulus of the experimental PR signal at λ = 374 nm obtained from nanometer scale implanted layers in Si, as a function of ultra-shallow junction depth.

Fig. 5 shows the modulus of the experimental PR signal for the "as implanted" samples, as a function of junction depth. For each junction depth, the modulus of the PR signal $|\Delta R/R|$ *decreases* approximately one order of magnitude for a two decade change in dose. This demonstrates good sensitivity to implant dose (prior to annealing) for the ultra-shallow junctions under consideration. The decrease in the signal with increasing dose is due to the damage from the implant reducing the sharpness of the crystalline Si E_1 critical point. This also accounts for the decreasing PR response with implant depth. This behavior of the PR signal is opposite that observed for the annealed wafers, and provides a clear method of distinction between active and inactive dopant. Additionally, it is seen each of the three "rows" in Fig. 5 exhibit the expected sinusoidal variation with junction depth.

CHARACTERIZATION OF STRAIN IN NANOMETER SCALE SI LAYERS

As mentioned, the underlying principle of the strain characterization technique is to measure small shifts in PR signals occurring near strong interband transitions in the semiconductor bandstructure. The silicon "E_1" interband transition occurring at $\lambda \cong 375$ nm is known to undergo a split and shift under strain according to: $E_{\pm} \cong E_1 + \Delta E_H \pm \Delta E_S$, where ΔE_H (< 0) and ΔE_S correspond to the hydrostatic and shear induced shifts, respectively [7]. Either term is linear in strain, leading to an overall shift linearly proportional to strain. For the Si strain levels of importance to the IC industry, and which are investigated herein, the magnitude of either term is approximately 50 meV [7]. This strain results in a redshift of the Si E_1 absorption by roughly 10 nm. By inspection of Fig. 2, it may be seen that a monochromatic PR probe beam located at $\lambda \cong 375$ nm will experience a change of sign of its response, from negative to positive, under just such a redshift. Further, in this vicinity, the PR signal is approximately linear in strain. Thus, by selecting a monochromatic probe beam with wavelength very near the Si E_1 transition, the measurement of strain may be accomplished according to a simple empirically determined correlation.

In order to demonstrate the PR based measurement of strain, two sample sets containing nanoscale strained silicon layers on silicon-germanium substrates were analyzed. S-Si sample set 1 contained five wafers: an unstrained silicon substrate; two unstrained silicon-germanium substrates (18.5% Ge); and two wafers with nanometer scale strained silicon films of approximately 6 nm thickness on top of unstrained silicon-germanium substrates (18.5% Ge). S-Si sample set 2 contained six wafers: each comprising nanometer scale silicon films on SiGe substrates, with variations in top silicon thickness and Ge concentration. Sample set 2 is described in Table 1.

TABLE 1. Strained Si on SiGe: Sample Set 2.

Wafer no.:	#1	#2	#3	#4	#5	#6
Filmstack:	Strained-Si/ SiGe substrate					
Ge [%]:	~15	~20	~20	~20	~15	~20
S-Si [nm]:	~20	~10	~10	~10	~15	~30

Fig. 6 shows the PR data taken on S-Si sample set 1, at a modulation frequency of 20 MHz. Wafers no.'s 1, 3, and 5, the unstrained silicon substrate and unstrained SiGe substrates, show PR signals of around

-1×10^{-5}. However, wafer no.'s 2 and 4, the wafers with top silicon of approximately 6 nm, show PR signals of opposite sign. Since the PR spectra is a linear superposition of the response from the top silicon film and the relaxed SiGe layers, we can deduce that if wafer no.'s 2 and 4 contained unstrained top silicon, the response of these wafers must be negative, similar to wafer no.'s 1, 3, and 5. Further, we have checked that the change of sign seen for wafer no.'s 2 and 4 cannot be a filmstack effect, due to the fact that the Seraphin coefficients do not change sign over the known filmstructure variations. Therefore, we assign the positive PR signals seen for wafer no.'s 2 and 4 to the presence of strain in the top silicon, in accordance with the described measurement principle.

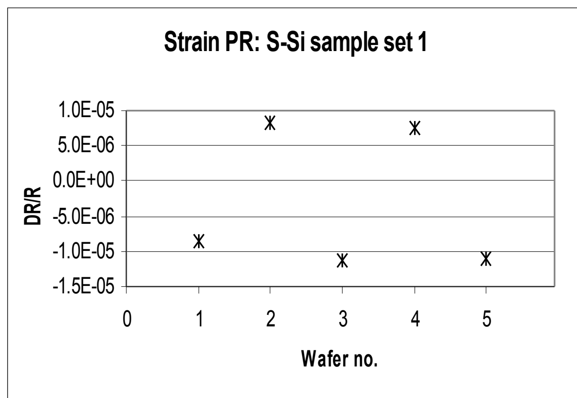

FIGURE 6. Measured PR signal at λ = 374nm obtained from ultra-thin strained Si layers on SiGe, plotted for each wafer in S-Si sample set 1.

Fig. 7 shows the PR data taken on S-Si sample set 2, at a modulation frequency of 20 MHz. Wafer no.'s 1, 5, and 6 each show negative PR signals of magnitude $\sim1\text{–}2\times10^{-5}$. However, wafer no.'s 2, 3, and 4 show PR signals of *opposite* sign, with magnitude $\sim3\times10^{-5}$. By examination of Table 2, it may be seen the positive PR signals correspond to wafers with top silicon film thicknesses of approximately 10 nm, while the negative signals correspond to films of thickness approximately 20 nm. This shows that for S-Si sample set 2, the strain becomes relaxed when the top silicon thickness exceeds approximately 20nm. This finding is supported by calculations predicting strain relaxation for top silicon films thicker than approximately 15 nm thickness under the conditions herein. We have also again confirmed the negative PR response cannot be a filmstack effect. Thus, in analogy with the results of sample set 1, we deduce that wafer no.'s 2, 3, and 4 of sample set 2 have strained top silicon films, while the other top silicon films are not strained. Therefore, in light of the established measurement precision, this new PR technique provides a highly sensitive and precise strain characterization capability suitable for process control of strain in nanometer scale silicon films.

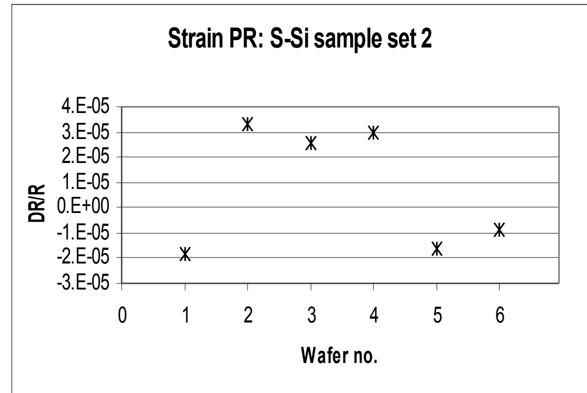

FIGURE 7. Measured PR signal at λ = 374nm obtained from ultra-thin strained Si layers on SiGe, plotted for each wafer in S-Si sample set 2 (shown in Table 1).

CONCLUSION

The PR technique discussed herein has been used for precision characterization of activated dopant in ultra-shallow junctions and precision characterization of strain in ultra-thin strained Si layers. This technique is for suitable for process control of electrically active semiconductor nanostructures and hence holds great promise as an enabling technology in the volume manufacture of nanoelectronics.

ACKNOWLEDGMENTS

W. Chism wishes to acknowledge and thank James Price and W. Lee Smith for many useful discussions regarding this work.

REFERENCES

1. B. O. Seraphin, *Phys. Rev.* **47**, A1716-A1725 (1965).
2. Peter Y. Yu and Manuel Cardona, *Fundamentals of Semiconductors*, Third Edition, Berlin: Springer, 2001.
3. Jon Opsal and Allan Rosencwaig, *Appl. Phys. Letters* **47**, 498-500 (1985).
4. David Sing (private communication).
5. Peter Borden, "Junction Depth Measurement using Carrier Illumination" in *Characterization and Metrology for ULSI Technology-2000*, edited by D. G. Seiler et al., AIP Conference Proceedings 550, American Institute of Physics, Melville, NY, 2001, pp. 175-180.
6. D. Aspnes, "Modulation Spectroscopy," in *Handbook on Semiconductors*, Vol. 2, edited by M. Balkanski, Amsterdam: North-Holland, 1980, pp. 109-154.
7. C. J. Vineis, *Phys. Rev. B* **71**, 245205 (2005).